

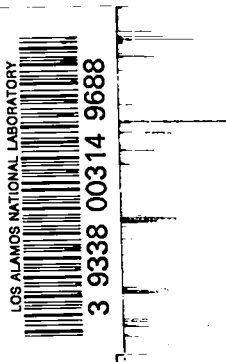
LA-3741

CS

CIC-14 REPORT COLLECTION  
**REPRODUCTION  
COPY**

**LOS ALAMOS SCIENTIFIC LABORATORY**  
of the  
**University of California**  
LOS ALAMOS • NEW MEXICO

**Nondestructive Detection, Identification,  
and Analysis of Fissionable Materials**



UNITED STATES  
ATOMIC ENERGY COMMISSION  
CONTRACT W-7405-ENG. 36

## LEGAL NOTICE

This report was prepared as an account of Government sponsored work. Neither the United States, nor the Commission, nor any person acting on behalf of the Commission:

A. Makes any warranty or representation, expressed or implied, with respect to the accuracy, completeness, or usefulness of the information contained in this report, or that the use of any information, apparatus, method, or process disclosed in this report may not infringe privately owned rights; or

B. Assumes any liabilities with respect to the use of, or for damages resulting from the use of any information, apparatus, method, or process disclosed in this report.

As used in the above, "person acting on behalf of the Commission" includes any employee or contractor of the Commission, or employee of such contractor, to the extent that such employee or contractor of the Commission, or employee of such contractor prepares, disseminates, or provides access to, any information pursuant to his employment or contract with the Commission, or his employment with such contractor.

This report expresses the opinions of the author or authors and does not necessarily reflect the opinions or views of the Los Alamos Scientific Laboratory.

Printed in the United States of America. Available from  
Clearinghouse for Federal Scientific and Technical Information  
National Bureau of Standards, U. S. Department of Commerce  
Springfield, Virginia 22151

Price: Printed Copy \$3.00; Microfiche \$0.65

**LOS ALAMOS SCIENTIFIC LABORATORY**  
**of the**  
**University of California**  
LOS ALAMOS • NEW MEXICO

Report written: January 1967

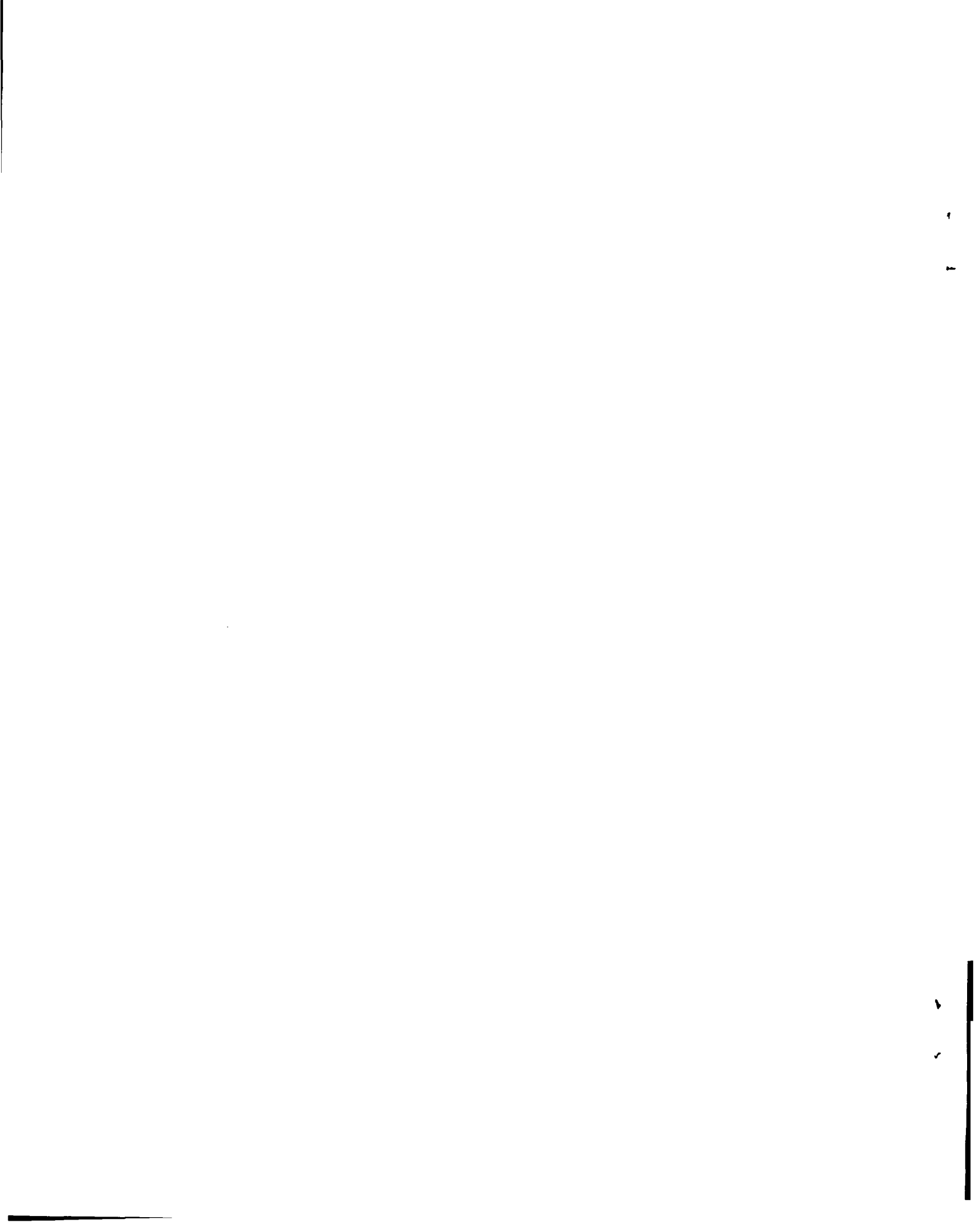
Report distributed: November 20, 1967

**Nondestructive Detection, Identification,**  
**and Analysis of Fissionable Materials**

by

G. Robert Keepin





NONDESTRUCTIVE DETECTION, IDENTIFICATION,  
AND ANALYSIS OF FISSIONABLE MATERIALS

by

G. Robert Keepin

ABSTRACT

Characteristic differences in relative group yields and energy spectra of delayed neutrons from the various fission species are used to provide unique methods for nondestructive detection, identification, and analysis of unknown mixtures of fissionable materials. Basically, these methods consist of detailed analysis (in time and, as a further refinement, in energy) of the measured delayed neutron activity from an unknown system following fast neutron irradiation. It is shown that such delayed neutron kinetic response measurements are largely free of the interfering and distorting effects inherent in other methods of detection and analysis.

Besides practical applications to isotope identification and quantitative analysis in mixed systems, the present methods are shown to be especially sensitive to fissile versus fertile ( $k_{\infty} < 1$ ) fissionable materials--a distinction of practical importance in nuclear safeguards inspection and surveillance techniques. Full exploitation of the methods outlined herein promises a wide range of applications in the nuclear industry as well as in the emerging field of national and international nuclear safeguards and atomic energy control.

---

INTRODUCTION

In view of the growing necessity for more comprehensive and effective national and international control of nuclear materials, the field of nuclear safeguards is destined to assume major importance in the era of widespread nuclear power proliferation (and the concomitant proliferation of fissile materials) which lies just ahead.

The most important technical requirement

for nuclear safeguards implementation is a non-destructive, direct physical means or technique of detecting, identifying, and quantitatively analyzing fissionable materials in unknown mixtures of fissionable and nonfissionable materials.

Four prime requisites of such a technique are:

- (1) high "penetrability," for complete assay capability throughout the entire volume of high-density bulk media; e. g., fissionable

material in various bulk forms, such as fuel elements, ingots, slugs, slurries, melts, and process solutions;

(2) "environment insensitivity," to enable operation in the presence of extremely high radiation fields, extraneous or inert bulk materials, various perturbations, background "noise," spurious signals, etc.;

(3) high "isotope discrimination power," to distinguish unequivocally and quantitatively between the various fissile and fertile species in a given unknown bulk mixture; and

(4) the technique(s) should be nondestructive, accurate, and reliable, and the equipment should be relatively simple, compact, and adaptable to a variety of applications (e. g., direct, on-line isotopic assay in fuel re-processing and fuel fabrication plants, and fuel handling and shipping facilities).

Techniques based on analyses of delayed neutron kinetic response to fast neutron irradiations (pulsed, modulated, or continuous) appear to offer the greatest promise of meeting the four very stringent requirements just outlined. The delayed neutron kinetic response methods described herein utilize the characteristic differences in relative group yields and energy spectra of delayed neutrons from the various fission isotopes to provide a sensitive, unique means of discrimination between the various fission species.

#### DELAYED NEUTRON KINETIC RESPONSE METHODS

The decay of delayed neutron activity<sup>(1)</sup> following neutron-induced fission of various fission species (isotopes) has been measured and analyzed into six major groups based on their decay periods, which range from ~0.2 to ~55 sec. Although the six group periods are similar (but not identical) for all the major species undergoing

neutron-induced fission, marked differences have been observed<sup>(2)</sup> in relative group abundances and energy spectra of delayed neutrons from the major fissioning species.

By examination of the mass and charge distributions of the major fissioning species, these delayed neutron yield and spectral differences have been correlated<sup>(2)</sup> with the known variation of average fission chain length from one fissioning isotope to another. Thus, the longer average  $\beta$ -decay chain lengths in fission of the high-neutron/proton-ratio species (e. g.,  $^{238}\text{U}$  and  $^{232}\text{Th}$ ) account for increased yields of particular (especially short period) delayed neutron precursors that exhibit minor or negligible yields in fission of the shorter chain-length, (low-neutron/proton-ratio) species, such as  $^{233}\text{U}$  and  $^{239}\text{Pu}$ . This "chain-length effect" is most apparent among the short-period delayed neutron groups; i. e., the increase of fission chain lengths in the sequence  $^{233}\text{U}$ ,  $^{239}\text{Pu}$ ,  $^{240}\text{Pu}$ ,  $^{235}\text{U}$ ,  $^{232}\text{Th}$ , and  $^{238}\text{U}$  fission correlates directly with increasing absolute yield of the fifth and sixth (shortest) delayed neutron groups through the sequence from  $^{233}\text{U}$  to  $^{238}\text{U}$  (see Tables 4-7 and 4-15 in Ref. 2).

These differences in delayed neutron yield (as well as associated spectral differences to be discussed later) are uniquely characteristic of the individual fission species, and can be exploited to provide a unique method for nondestructive detection, identification, and analysis of individual fission isotopes in unknown mixtures of fissionable and nonfissionable materials.

The major technique described herein involves irradiating a system or sample of unknown composition with an intense, short pulse of neutrons (i. e., pulse duration short compared to all delayed neutron periods,  $\tau_1$ ), and analyzing the measured kinetic behavior of delayed neutron activity following the pulse. Modulated or continuous (i. e., saturation) irradiations may be

similarly analyzed to provide data complementary to that obtained by the pulsed technique. As will be seen below, the short-pulse irradiations generally provide optimum discrimination between the delayed neutron response curves of the different fissioning species.

#### ANALYSIS BY TIME-FIDUCIAL TECHNIQUES

To outline the analytical basis of delayed neutron kinetic response methods, we start with the delayed neutron emission function  $D(t)$  (see Ref. 2), which expresses the time dependence of delayed neutron activity following an instantaneous neutron irradiation (irradiation time,  $T \ll \tau_i$ ) producing  $\dot{F}T$  fissions in the irradiated sample:

$$D(t) = (\beta\bar{\nu}) \dot{F}T \sum_{i=1}^6 a_i \lambda_i e^{-\lambda_i t}. \quad (1)$$

Here,  $\beta\bar{\nu}$  (sometimes designated  $n/F$ ) is the absolute yield of delayed neutrons per fission and  $a_i \lambda_i$  are the measured abundances and decay constants, respectively, of the delayed neutron groups for a given fissioning species. We wish to compare the numbers of delayed neutrons emitted in various time intervals following both short (or "instantaneous") and saturation irradiations. First, we consider a single fission species; later the results will be generalized to mixtures of several different fission species.

The number of delayed neutrons emitted between the end of irradiation,  $t = 0$ , and an arbitrary time fiducial,  $f$ , following an instantaneous irradiation is

$$\begin{aligned} \int_0^f D(t) dt &= (\beta\bar{\nu}) \dot{F}T \int_0^f \sum_i a_i \lambda_i e^{-\lambda_i t} dt \\ &= (\beta\bar{\nu}) \dot{F}T \sum_i a_i \left( 1 - e^{-\lambda_i f} \right). \end{aligned} \quad (2)$$

For the special cases of very short and very long\* counting times, Eq. 2 reduces to

$$\begin{aligned} \int_0^f D(t) dt &\rightarrow (\beta\bar{\nu}) \dot{F}T f \sum_i a_i \lambda_i \quad \text{for } f \ll \tau_i; \\ &\rightarrow (\beta\bar{\nu}) \dot{F}T \quad \text{for } f \gg \tau_i. \end{aligned} \quad (3)$$

It follows that the fraction,  $R_{f-}$ , of delayed neutrons emitted in the interval  $0 < t < f$  following an instantaneous irradiation is given by

$$\begin{aligned} R_{f-} &= \frac{\int_0^f D(t) dt}{\int_0^\infty D(t) dt} = \frac{(\beta\bar{\nu}) \dot{F}T \sum_i a_i \left( 1 - e^{-\lambda_i f} \right)}{(\beta\bar{\nu}) \dot{F}T} \\ &= \sum_i a_i \left( 1 - e^{-\lambda_i f} \right). \end{aligned} \quad (4)$$

For later use we introduce the complementary fraction

$$R_{f+} = 1 - R_{f-} = \sum_i a_i e^{-\lambda_i f}, \quad (5)$$

which is simply the fraction of delayed neutrons emitted after time fiducial  $f$ ; i. e., in the interval  $f < t < \infty$ .

Turning to the case of saturation irradiations, the emission function  $D_S(t)$  (see Ref. 2) represents delayed neutron activity as a function of time following a saturation irradiation (irradiation time,  $T \gg \tau_i$ ) at constant fission rate,  $\dot{F}$ :

\*The case  $\int_0^\infty D(t) dt \rightarrow (\beta\bar{\nu}) \dot{F}T$  is the basis of the prompt-burst method of measuring absolute delayed neutron yields. (2) This method, developed at the Los Alamos Scientific Laboratory, has been used to measure absolute delayed neutron yields in fast and thermal fission of all the main fission species of practical interest.

$$D_S(t) = (\beta\bar{\nu}) \dot{F} \sum_i a_i e^{-\lambda_i t}. \quad (6)$$

Hence, the number of delayed neutrons emitted in the time interval  $0 < t < f$  following a saturation irradiation is

$$\begin{aligned} \int_0^f D_S(t) dt &= (\beta\bar{\nu}) \dot{F} \int_0^f \sum_i a_i e^{-\lambda_i t} dt \\ &= (\beta\bar{\nu}) \dot{F} \sum_i \left( \frac{a_i}{\lambda_i} \right) \left( 1 - e^{-\lambda_i f} \right), \end{aligned} \quad (7)$$

which reduces to

$$\begin{aligned} \int_0^f D_S(t) dt &\rightarrow (\beta\bar{\nu}) \dot{F} f \quad \text{for } f \ll \tau_i; \\ &\rightarrow (\beta\bar{\nu}) \dot{F} \sum_i a_i / \lambda_i \quad \text{for } f \gg \tau_i. \end{aligned} \quad (8)$$

The fraction,  $S_f$ , of delayed neutrons emitted in  $0 < t < f$  following a saturation irradiation is given by

$$\begin{aligned} S_f &\equiv \frac{\int_0^f D_S(t) dt}{\int_0^\infty D_S(t) dt} \\ &= \frac{(\beta\bar{\nu}) \dot{F} \sum_i (a_i / \lambda_i) \left( 1 - e^{-\lambda_i f} \right)}{(\beta\bar{\nu}) \dot{F} \sum_i a_i / \lambda_i}, \end{aligned} \quad (9)$$

which reduces to

$$\begin{aligned} S_f &\rightarrow \frac{(\beta\bar{\nu}) \dot{F} f}{(\beta\bar{\nu}) \dot{F} \sum_i a_i / \lambda_i} = \frac{f}{\sum_i a_i / \lambda_i} \quad \text{for } f \ll \tau_i; \\ &\rightarrow \text{unity} \quad \text{for } f \gg \tau_i. \end{aligned} \quad (10)$$

We now extend the previous definitions of  $R_{f-}$  and  $S_f$  for a single fission isotope to the corresponding functions  $\bar{R}_{f-}$  and  $\bar{S}_f$  for a mixture of different fission species\* denoted by the index  $q$ . Thus, for instantaneous irradiations, Eq. 4 may be generalized as follows:

$$\bar{R}_{f-} = \frac{\sum_q (\beta\bar{\nu})^q \dot{F}^q T \sum_i a_i^q \left( 1 - e^{-\lambda_i^q f} \right)}{\sum_q (\beta\bar{\nu})^q \dot{F}^q T} \quad (11)$$

which is simply a weighted sum of the known delayed neutron kinetic functions

$$\sum_i a_i^q \left( 1 - e^{-\lambda_i^q f} \right)$$

for each isotope,  $q$ ; the weighting factor is the fractional delayed neutron yield, or production, from each isotope. For the special case of very short  $f$ , Eq. 11 reduces to

$$\bar{R}_{f-} \rightarrow \frac{\sum_q (\beta\bar{\nu})^q \dot{F}^q f \sum_i a_i^q \lambda_i^q}{\sum_q (\beta\bar{\nu})^q \dot{F}^q} \quad \text{for } f \ll \tau_i, \quad (12)$$

which again is simply a weighted sum of the known functions  $\sum_i a_i \lambda_i$  for each isotope. From measured delayed neutron decay characteristics for all the major fission species, precise numerical values of  $\sum_i a_i \lambda_i$  and their propagated errors, as well as the first and second moments of the delayed neutron decay constants and mean lives, have recently been determined for all major fission species (see Table 10-1 of Ref. 2).

\*In general, the number of major fissioning species in a given system or device will not exceed three.



For saturation irradiations, Eq. 9 may be generalized as follows:

$$\bar{S}_f \rightarrow \frac{\sum_q (\beta\bar{\nu})^q \dot{F}^q \sum_i a_i^q / \lambda_i^q (1 - e^{-\lambda_i^q f})}{\sum_q (\beta\bar{\nu})^q \dot{F}^q \sum_i a_i^q / \lambda_i^q} \quad (13)$$

For the special case of very short  $f$ , Eq. 13 reduces to

$$\bar{S}_f \rightarrow \frac{\sum_q (\beta\bar{\nu})^q \dot{F}^q f}{\sum_q (\beta\bar{\nu})^q \dot{F}^q \sum_i a_i^q / \lambda_i^q} \quad \text{for } f \ll \tau_i, \quad (14)$$

and the reciprocal of  $\bar{S}_f$  is again a delayed-neutron-yield weighted sum of the known kinetic functions,  $\sum_i a_i^q / \lambda_i^q$ .

Since the expression  $\bar{S}_f$  given in Eq. 13 does not lend itself to isotope analysis applications, an alternative formulation is the ratio,  $\bar{S}_{f^-/\Delta}$ , of delayed neutrons emitted in the time interval  $0 < t < f$  following a saturation irradiation to those emitted in a fixed, short time interval  $\Delta \ll \tau_i$  following the irradiation:

$$\bar{S}_{f^-/\Delta} = \frac{\sum_q (\beta\bar{\nu})^q \dot{F}^q \sum_i (a_i^q / \lambda_i^q) (1 - e^{-\lambda_i^q f})}{\Delta \sum_q (\beta\bar{\nu})^q \dot{F}^q} \quad (15)$$

We also introduce the complementary ratio,  $\bar{S}_{f^+/\Delta}$ , for delayed neutrons emitted after time fiducial  $f$ :

$$\bar{S}_{f^+/\Delta} = \frac{\sum_q (\beta\bar{\nu})^q \dot{F}^q \sum_i (a_i^q / \lambda_i^q) e^{-\lambda_i^q f}}{\Delta \sum_q (\beta\bar{\nu})^q \dot{F}^q} \quad (16)$$

These expressions have the desired tractable form of a weighted sum of known delayed neutron kinetics functions for each isotope,  $q$ , the weighting function being, as before, the fractional delayed neutron production from each fissioning species.

Letting  $[W]$  symbolize the process of weighting with fractional delayed neutron production from each fission species present in a given mixture, the preceding development can be summarized as follows:

For Burst Irradiations:

$$\bar{R}_{f^-} = [W] \sum_i a_i (1 - e^{-\lambda_i f});$$

$$\bar{R}_{f^+} = [W] \sum_i a_i e^{-\lambda_i f}. \quad (17)$$

For Saturation Irradiations:

$$\bar{S}_{f^-/\Delta} = \Delta^{-1} [W] \sum_i a_i / \lambda_i (1 - e^{-\lambda_i f});$$

$$\bar{S}_{f^+/\Delta} = \Delta^{-1} [W] \sum_i a_i / \lambda_i e^{-\lambda_i f}. \quad (18)$$

Limiting values of these functions for very small and very large values of  $f$  are given in Table I.

As noted above, precise numerical values of  $\sum_i a_i \lambda_i$  and  $\sum_i a_i / \lambda_i$  have recently been determined, together with their least-squares propagated uncertainties, for all the major fission species. <sup>(2)</sup> These data are included in Table II, which gives first and second moments of the delayed neutron decay constants and mean lives.

The  $\bar{R}_f$  (burst-response) functions emphasize the shorter-period delayed neutron groups, and the  $\bar{S}_f$  (saturation-response) functions emphasize the longer-period groups. This capability for selective emphasis of both extremes of the de-

layed neutron period spectrum provides two complementary time-fiducial methods for identification and analysis of individual fission isotopes. Intermediate cases (i. e., between pulsed and saturation irradiations) are readily obtained by using modulated neutron sources.

TABLE I

Limiting Values of Kinetic Functions

$f \ll \tau_i$	Quantity	$f \gg \tau_i$
$f[W] \sum_i a_i \lambda_i$	$\overline{R}_{f-}$	1
1	$\overline{R}_{f+}$	0
$f/\Delta$	$\overline{S}_{f-\Delta}$	$\Delta^{-1}[W] \sum_i a_i / \lambda_i$
$\Delta^{-1}[W] \sum_i a_i / \lambda_i$	$\overline{S}_{f+\Delta}$	0
$f \left\{ [W] \sum_i a_i / \lambda_i \right\}^{-1}$	$\overline{S}_f$	1

From the preceding development it follows that measured values of  $\overline{R}_f$  (and also  $\overline{S}_{f/\Delta}$  when desired) for various time fiducial values,  $f$ , can be used to determine fractional delayed neutron production from each major fission isotope in a given mixture of fissioning species. In such an analysis, a linear superposition of known kinetic functions (e. g.,  $\sum_i a_i (1 - e^{-\lambda_i f})$  in the case of  $\overline{R}_{f-}$  measurements) with unknown coefficients (fractional delayed neutron yields) is obtained in each time interval. The number of simultaneous equations in these coefficients (i. e., number and range of time intervals) can be judiciously chosen, for a given application, to suit the precision of the experimental data and to optimize the sensitivity and accuracy of the analysis.

To indicate generally the capabilities and accuracy of the time-fiducial method, we examine the dependence of  $R_f$  and  $S_{f/\Delta}$  functions on  $f$ .

TABLE II

Moments of Delayed-Neutron Mean-Lives and Decay Constants

(Computed, with least-squares propagated uncertainties, from data of Table 4-7, Ref. 2)

	$^{235}\text{U}$	$^{233}\text{U}$	$^{239}\text{Pu}$
$\sum a_i / \lambda_i (\text{sec})$	12.753 ± 0.1834	17.876 ± 0.2866	14.6445 ± 0.1698
$\sum a_i \lambda_i (\text{sec}^{-1})$	0.4353 ± 0.0109	0.3004 ± 0.0194	0.3888 ± 0.0126
$\sum a_i / \lambda_i^2 (\text{sec}^2)$	466.05 ± 12.643	804.07 ± 22.302	532.94 ± 10.957
$\sum a_i \lambda_i^2 (\text{sec}^{-2})$	0.682 ± 0.0464	0.376 ± 0.065	0.564 ± 0.042
	$^{240}\text{Pu}$	$^{238}\text{U}$	$^{232}\text{Th}$
$\sum a_i / \lambda_i (\text{sec})$	13.467 ± 0.2624	7.6803 ± 0.1025	10.059 ± 0.1657
$\sum a_i \lambda_i (\text{sec}^{-1})$	0.4426 ± 0.0255	0.7847 ± 0.0179	0.5169 ± 0.0165
$\sum a_i / \lambda_i^2 (\text{sec}^2)$	460.68 ± 11.636	219.10 ± 4.313	370.62 ± 8.965
$\sum a_i \lambda_i^2 (\text{sec}^{-2})$	0.753 ± 0.111	1.712 ± 0.080	0.766 ± 0.057

Computer calculations\* of  $R_{f-}$  and  $R_{f+}$  versus  $f$  are plotted in Fig. 1 for  $^{235}\text{U}$ ,  $^{238}\text{U}$ ,  $^{233}\text{U}$ , and  $^{239}\text{Pu}$ . Each  $R_{f-}$  curve approaches its limiting value,  $f \sum_i a_i \lambda_i$  for small  $f$ . Relative magnitudes of  $R_{f-}$  values (and  $R_{f+}$  values, as well) for the different isotopes are clearly an index of the sensitivity or the isotope discrimination power of the  $\overline{R}_f$  method. Ratios of  $R_{f-}$  and  $R_{f+}$  values--"isotope discrimination ratios"--as a function of  $f$  are shown in Fig. 2, where appropriate limiting values are again indicated for small  $f$ . Optimum isotope discrimination in  $R_{f-}$  measurements is obtained in the range of small  $f$  values ( $< 0.1$  sec), while optimum discrimination in  $R_{f+}$  measurements is obtained at the larger  $f$  values ( $> 10$  sec).

The ratios  $R_{f-}/R_{f+}$  for each species can be used to provide still greater discrimination between individual species, as will be discussed below. It may be noted here that such ratios, e. g.,  $R_{f-}(0.1 \text{ sec})/R_{f+}(50 \text{ sec})$ , constitute a measure of the average delayed neutron decay "slopes" (early to late neutron emission) for the individual species.

Computer calculations of the kinetic functions  $\Delta \cdot S_{f+\Delta}$  and  $\Delta \cdot S_{f-\Delta}$  versus  $f$  (see Eq. 18) are plotted in Fig. 3 for  $^{235}\text{U}$ ,  $^{238}\text{U}$ ,  $^{233}\text{U}$ , and  $^{239}\text{Pu}$ . Appropriate limiting values,  $\sum_i a_i/\lambda_i$ , are indicated at large and small  $f$ . Ratios of  $S_{f+\Delta}$  values are plotted in Fig. 4. The  $S_{f-\Delta}$  ratios are not plotted as they are generally too small to be of practical interest, i. e., because their maximum limiting value is  $\sum_i a_i/\lambda_i$  at large  $f$ , which is just the limiting minimum value of  $S_{f+\Delta}$  ratios at small  $f$ .

In the respective time regions of their maximum values,  $R_{f-}$  and  $R_{f+}$  ratios emphasize completely different extremes of the delayed neutron

period-spectrum, and hence constitute essentially independent measurements. Accordingly, we multiply optimum ratio values (from Figs. 2 and 4) together to obtain "effective discrimination factors" for various pairs of isotopes (see Table III). These factors are simply ratios of delayed-neutron-decay slopes as defined previously for the individual species.

It is noteworthy that an effective discrimination factor as large as 10 is obtainable between the uranium isotopes  $^{238}\text{U}$  and  $^{233}\text{U}$ , a factor of 5 between  $^{238}\text{U}$  and  $^{239}\text{Pu}$ ,\* and a factor of over 3 between  $^{238}\text{U}$  and  $^{235}\text{U}$ . The smallest discrimination factor ( $\sim 1.4$ ) is obtained between  $^{235}\text{U}$  and  $^{239}\text{Pu}$ . Figures 2 and 4 show that still higher discrimination factors between all combinations of isotopes in Table III (except  $^{239}\text{Pu}$  and  $^{235}\text{U}$ ) are possible using  $f$  values larger than 50 sec. In some cases, however, the available delayed neutron intensity may limit the statistical accuracy of  $R_{f+}$  or  $S_{f+\Delta}$  measurements for  $f > 50$  sec. (See later discussion of experimental technique and accuracy of measurements.)

Before any analysis of relative amounts of fissionable material can be carried out, the major fission isotopes present in a given system must first be identified. Consider the response to fast-neutron (14 MeV) pulsed irradiations. Figure 1 shows that the presence of  $^{238}\text{U}$  as a major fissioning species will be indicated by measured  $\overline{R}_{f-}$  values in excess of the corresponding  $R_{f-}(^{235}\text{U})$  by more than a few percent. The same conclusion holds if measured  $\overline{R}_{f+}$  is less than  $R_{f+}(^{235}\text{U})$  by more than a few percent.

\* Calculations are based on experimental delayed neutron decay data;<sup>(2)</sup> Los Alamos prompt-burst decay data for all the major fission species are available in computer-listing form.

\* Similarly excellent discrimination is obtainable between  $^{233}\text{U}$  and  $^{232}\text{Th}$ ; the  $\overline{R}_f$  and  $\overline{S}_{f/\Delta}$  methods should find extensive practical applications to assay and burnup determinations in  $^{238}\text{U}$ - $^{239}\text{Pu}$  breeders as well as to  $^{232}\text{Th}$ - $^{233}\text{U}$  systems. Also, the large effective discrimination factor between  $^{235}\text{U}$  and  $^{238}\text{U}$  recommends the present methods for rapid, nondestructive determination of isotopic abundances in enriched uranium fuel or feed material.

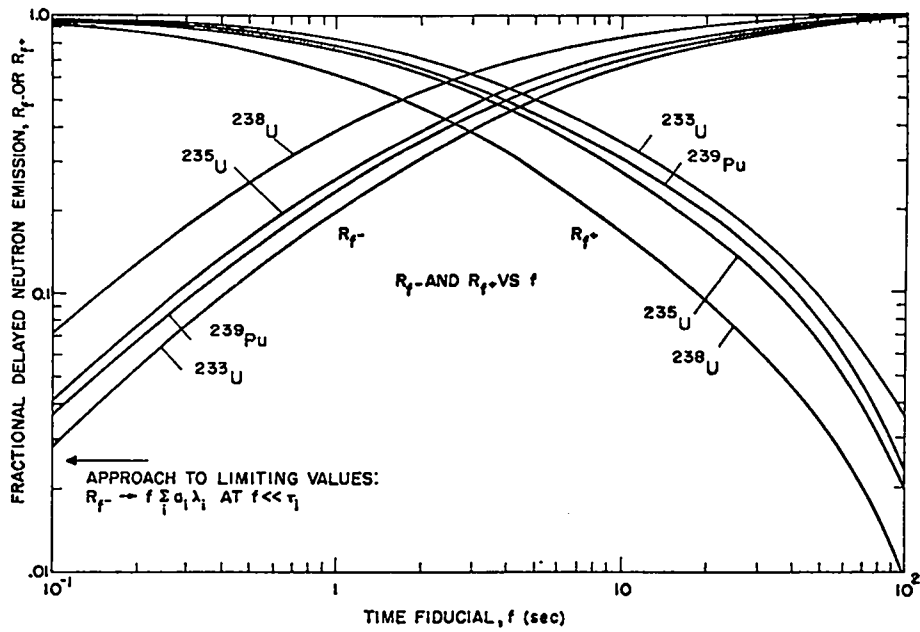


Fig. 1.  $R_{f-}$  and  $R_{f+}$  functions for various fission species plotted against the variable time fiducial,  $f$ .

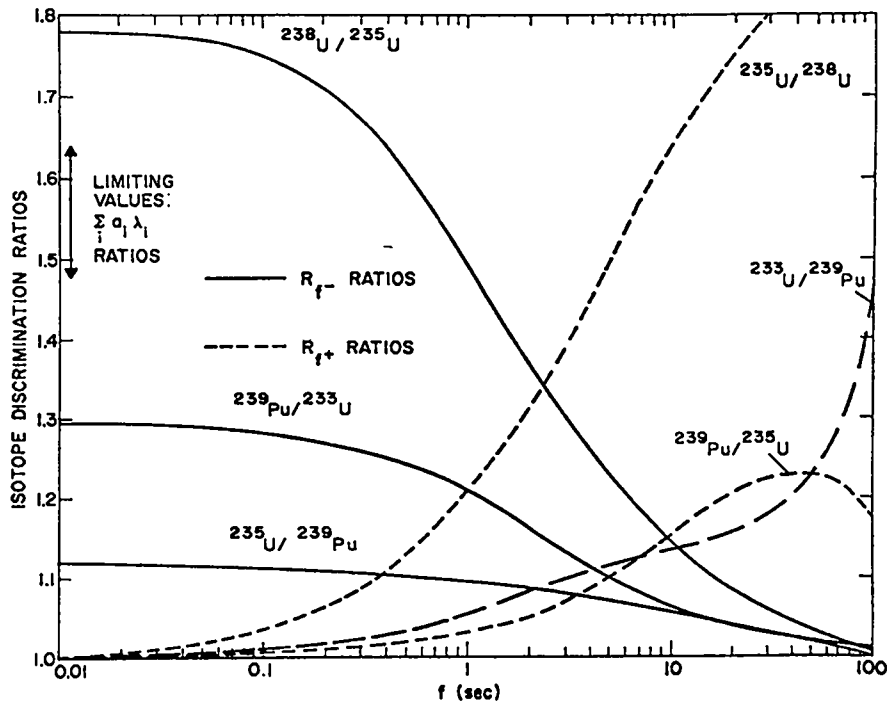


Fig. 2. Isotope discrimination ratios ( $R_{f-}$  and  $R_{f+}$  ratios) as a function of the variable time fiducial,  $f$ , for various combinations of isotopes.

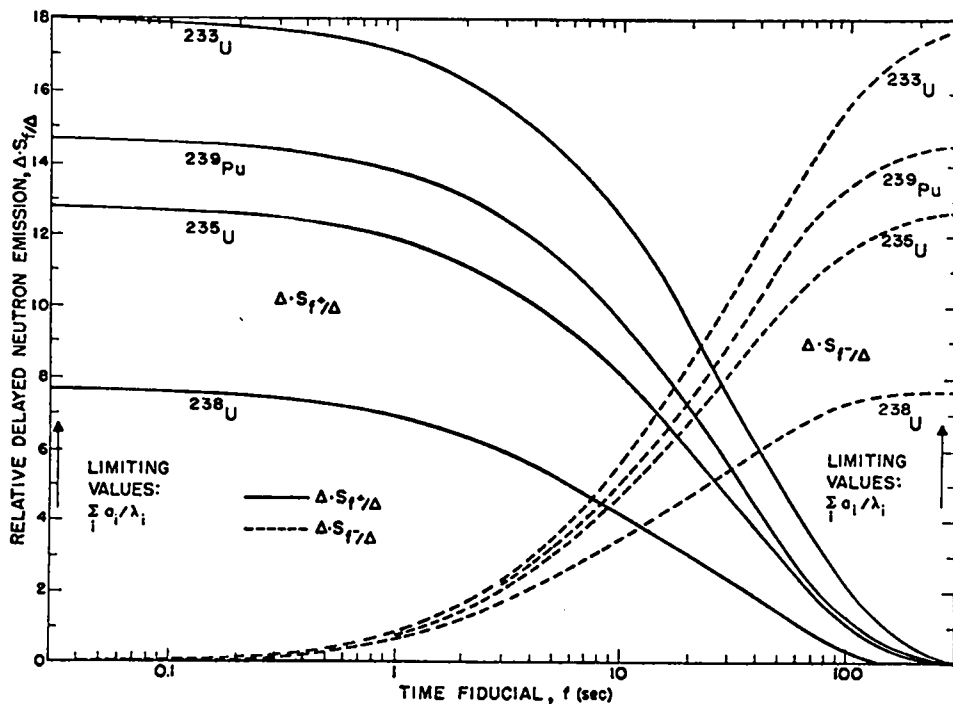


Fig. 3.  $\Delta \cdot S_{f+} / \Delta$  and  $\Delta \cdot S_{f-} / \Delta$  functions for various fission species plotted against the variable time fiducial,  $f$ .

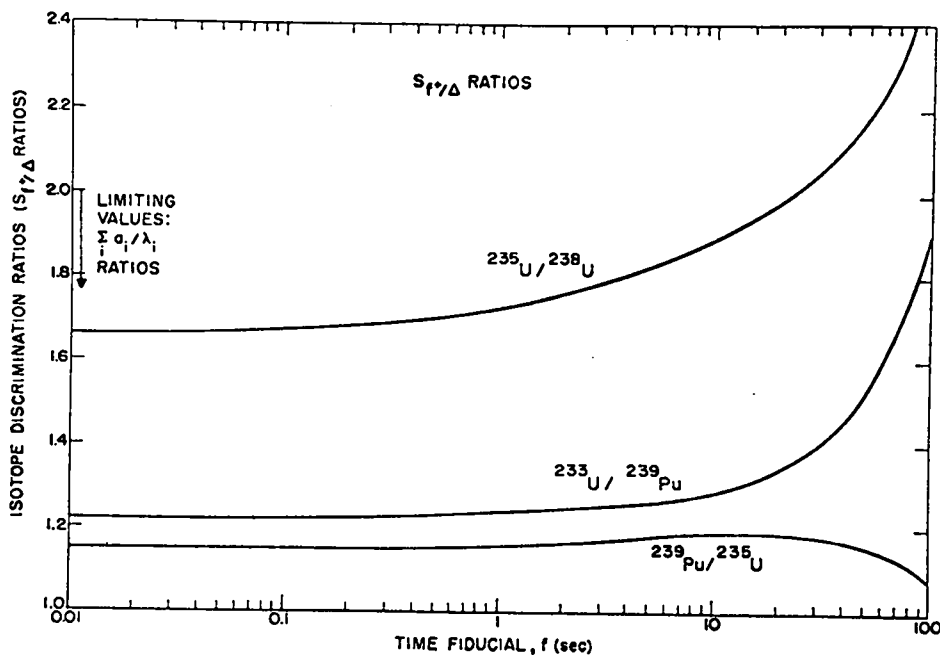


Fig. 4. Isotope discrimination ratios ( $S_{f+} / \Delta$  ratios) as a function of the variable time fiducial,  $f$ , for various combinations of isotopes.

TABLE III

## Effective Isotope Discrimination Factors

Obtained from  $R_{f-}$ ,  $R_{f+}$ , and  $S_{f+}/\Delta$  Measurements

Isotopes	$R_{f-}$ Ratio (f=0.1 sec)	$R_{f+}$ Ratio (f=50 sec)	Effective Discrimination Factor ( $R_{f-}$ and $R_{f+}$ )	$S_{f+}/\Delta$ Ratio (f=50 sec)	Effective Discrimination Factor ( $R_{f-}$ and $S_{f+}/\Delta$ )
$^{238}\text{U}$ , $^{235}\text{U}$	1.75	1.88	3.30	2.18	3.80
$^{238}\text{U}$ , $^{239}\text{Pu}$	2.0	2.3	4.60	2.60	5.2
$^{238}\text{U}$ , $^{233}\text{U}$	2.56	2.85	7.30	4.0	10.2
$^{235}\text{U}$ , $^{239}\text{Pu}$	1.12	1.23	1.38	1.19 <sup>a</sup>	1.33
$^{235}\text{U}$ , $^{233}\text{U}$	1.42	1.52	2.15	1.82	2.60
$^{239}\text{Pu}$ , $^{233}\text{U}$	1.28	1.23	1.58	1.52	1.94

<sup>a</sup>at f = 20 sec.

In specific numerical terms this means, for example, that  $^{238}\text{U}$  is present if measured  $\overline{R_{f-}} \gtrsim 0.045$  at f = 0.1 sec or if  $\overline{R_{f+}} \lesssim 0.06$  at f = 50 sec. Similarly, for saturation irradiations in Fig. 3, if measured  $\Delta \cdot \overline{S_{f+}/\Delta}$  is less than  $\sim 12$  for f  $\lesssim 0.5$  sec, then  $^{238}\text{U}$  is present as a major fissioning species.

Identification of individual species can be carried out more effectively on the basis of  $R_{f-}/R_{f+}$  ratios (delayed neutron decay slopes) for the individual species. Table IV gives numerical values of these slopes for the time fiducials 0.1 and 50 sec. Delayed neutron decay slopes--being a combination of  $R_{f-}$  and  $R_{f+}$  values--provide a more sensitive measurable characteristic of individual fission species than either  $R_{f-}$  or  $R_{f+}$  values alone. In specific numerical terms, if the observed slope,  $R_{f-}(0.1 \text{ sec})/R_{f+}(50 \text{ sec})$ , of an unknown mixture of fissioning materials exceeds 0.7, for example, the presence of  $^{238}\text{U}$  is indicated (see Table IV). Similarly, the presence of  $^{233}\text{U}$  is indicated if measured delayed neutron decay slope falls below  $\sim 0.44$ . In systems where

$^{233}\text{U}$  is not present (which in fact applies to nearly all practical cases), a measured decay slope less than  $\sim 0.60$  would indicate the presence of  $^{239}\text{Pu}$ .

From a practical standpoint, the actual degree of discrimination ultimately obtainable between fission species as similar as  $^{235}\text{U}$  and  $^{239}\text{Pu}$  (which exhibit the smallest difference in delayed neutron kinetic characteristics) must be investi-

TABLE IV

Average Delayed Neutron Decay "Slopes"  
Characteristic of Individual Fission Species

Fission Species	$R_{f-}(0.1 \text{ sec})/$ $R_{f+}(50 \text{ sec})$
$^{238}\text{U}$	2.06
$^{235}\text{U}$	0.626
$^{239}\text{Pu}$	0.458
$^{233}\text{U}$	0.290

gated experimentally.\* Some alternative approaches to  $^{235}\text{U}$  vs  $^{239}\text{Pu}$  discrimination are possible, and warrant further careful and systematic investigation under both laboratory and field conditions.

In systems where identification by delayed neutron response alone is difficult, one may employ supplementary methods such as high-resolution gamma spectrometry for identification of individual isotopes (see Supplementary Methods).

Thorium-232 has been largely ignored here for several reasons. First,  $^{232}\text{Th}$  has nearly an order of magnitude smaller fission cross section for fast neutrons than do the other major fission species. Second, with the exception of the new large thorium reactors,  $^{232}\text{Th}$  is simply not used as a fissionable material in practical fission systems and devices. Its future use will likely be confined to large breeder and converter reactors, where its presence should certainly be well known. Nevertheless, in future  $^{232}\text{Th}$ - $^{233}\text{U}$ -cycle breeder reactors, the  $^{232}\text{Th}$  and  $^{233}\text{U}$  can be readily identified and analyzed by the delayed neutron response methods outlined herein. For example, from Table II one obtains good discrimination ratios between  $^{233}\text{U}$  and  $^{232}\text{Th}$  of 1.72 and 1.78 for  $R_{f-}$  and  $S_{f+\Delta}$  ratios, respectively, at small  $f$ ; and considerably larger discrimination ratios are available from  $R_{f+}$  and  $S_{f+\Delta}$  measurements at large  $f$  (see Figs. 2 and 4).

Separate neutron irradiations with subthreshold fast neutrons and with superthreshold fast neutrons can clearly be used to provide further discrimination between the fissile and the thres-

\* In certain inspection and surveillance applications, it is not always necessary to distinguish between  $^{239}\text{Pu}$  and  $^{235}\text{U}$  components in a given system, it being sufficient to determine the combined  $^{235}\text{U}$ - $^{239}\text{Pu}$  SNM (special nuclear material) contribution relative to the  $^{238}\text{U}$  fertile material ( $k_{\infty} < 1$ ) contribution in the system. Such an analysis is readily obtained through appropriate  $R_f$  and  $S_{f/\Delta}$  measurements. (For further details, see later discussion of Practical Applications.)

hold fissioning species, notably  $^{235}\text{U}$ ,  $^{239}\text{Pu}$ , and  $^{233}\text{U}$  vs  $^{238}\text{U}$ . (Fortunately for isotopic analysis applications, the delayed neutron parameters,  $a_i$  and  $\lambda_i$ , are not sensitive to the energy of the neutron inducing fission.)

In highly heterogeneous systems, there can arise perturbations due to differential self-shielding of delayed neutrons from the different fission species. Implicit in the present development is the assumption that a flat-energy-response detector "sees" all delayed neutrons from the system equally well. Fortunately, we are dealing with fast neutrons, so the assumption of system "transparency" is generally good, and high-efficiency, "flat-response" fast neutron detectors are readily available. Of course, problems are bound to arise in practical applications of delayed neutron kinetic response techniques to various types of complex, heterogeneous systems, and a systematic program of computational and experimental investigation of the full potential of these techniques applied to such systems is being undertaken at Los Alamos.

We now consider, by way of illustration, representative experimental conditions for typical pulsed irradiations of a mixture of fissionable materials. Modern, compact, pulsed neutron sources are capable of producing high yield, short pulses (short compared to  $\tau_i$ ) with time-average intensities well above  $10^{11}$  neutrons/sec using the  $\text{D}+\text{T} \rightarrow \text{n}+\text{He}^4$  reaction. Single pulse yields in excess of  $10^{12}$  n/pulse are readily attainable with current technology.<sup>(3)</sup> Such compact, intense pulsed neutron sources are being adapted specifically for delayed neutron kinetic response applications. Assuming reasonable geometrical coupling factors (e. g., 10%) between the source and the system and assuming nominal 1% neutron detection efficiency, \* adequate count-

\* Actually in multidetector  $4\pi$  counting geometries, 80% or higher overall efficiency is readily attainable.

ing statistics in neutron kinetic response measurements can normally be obtained in several minutes. In a given experimental situation, of course, the number of pulsed irradiations as well as the type and geometry of source(s) and detector(s) can be varied as necessary to achieve desired statistical accuracy in each f-defined time interval.

With a "flat"-energy-response neutron detector,  $\overline{R}_f$  values can be readily measured to considerably better than 1% statistical accuracy in reasonable counting times (usually in minutes, as already noted). The basic kinetic functions  $R_{f-}$ ,  $R_{f+}$ , and  $\Delta \cdot S_{f+/\Delta}$  are known to an accuracy of a few percent, as may be inferred from the uncertainties on the limiting forms  $\sum_i a_i \lambda_i$  and  $\sum_i a_i / \lambda_i$ . \* Values of  $(\beta\overline{v})^q$  are also known to a few percent accuracy. (2) Thus, the relative number of fissions of each major fissioning isotope present in an unknown mixture can be determined directly and quantitatively by kinetic response methods. Appropriate fission cross-section ratios can then be used to determine the relative amounts of each major fissioning isotope present.

As we have seen, the experimental techniques for measuring delayed neutron kinetic response are relatively straightforward and do not require expensive equipment. The method does not require either absolute detector calibration or absolute fission monitor counting (although in some cases fission ratio determinations, either calculated or measured, may be desirable to determine relative amounts of each major fission species present).

Since  $\beta$  decay is essentially forbidden for half lives shorter than  $\sim 0.1$  sec, delayed neutrons

\* In Table II the least-squares propagated uncertainties in  $\sum a_i \lambda_i$  range from 2.3% for  $^{238}\text{U}$  to 6.5% for  $^{233}\text{U}$ , with an average of  $\sim 3.6\%$  for all isotopes. The uncertainties in  $\sum a_i / \lambda_i$  range from 1.2% for  $^{239}\text{Pu}$  to 1.7% for  $^{232}\text{Th}$ , with an average of  $\sim 1.4\%$  for all isotopes.

are not expected, or observed, to exhibit half lives shorter than 0.1 sec. Thus, delayed neutron kinetic response methods offer the great advantage that all measurements are made in a time domain which is completely free of time-dependent perturbations due to prompt-neutron higher modes, thermalization and diffusion effects (confined to the sub-millisecond time region), neutron time-of-flight smear, etc. Further important advantages are: (1) "environment insensitivity" (to the presence of high radiation fields, inert and/or extraneous materials, etc.), and (2) the high "penetrability" of fast neutrons through bulk media.

#### ANALYSIS OF MULTICHANNEL-TIME-ANALYZER DATA

Equations 17 and 18 can be generalized to an arbitrary number of time intervals for analysis of multi-channel-time-analyzer decay data to obtain fractional delayed neutron production in a given system. The fraction  $\overline{R}_n$  of delayed neutrons emitted in the  $n^{\text{th}}$  time channel ( $t_{n-1} < t < t_n$ ) following an instantaneous irradiation is (see Eq. 11):

$$\overline{R}_n = \frac{\sum_q (\beta\overline{v})^q \dot{F}^q T \sum_i a_i (e^{-\lambda_i^q t_{n-1}} - e^{-\lambda_i^q t_n})}{\sum_q (\beta\overline{v})^q \dot{F}^q T} \quad (19)$$

Similarly, Eq. 15 is generalized to the multi-channel case:

$$\overline{S}_{n/\Delta} = \frac{\sum_q (\beta\overline{v})^q \dot{F}^q \sum_i a_i^q / \lambda_i^q (e^{-\lambda_i^q t_{n-1}} - e^{-\lambda_i^q t_n})}{\Delta \sum_q (\beta\overline{v})^q \dot{F}^q} \quad (20)$$



Thus, in general for  $q$  isotopes and  $n \geq q$  time intervals, a set of  $\overline{R}_n$  (or  $\overline{S}_{n/\Delta}$ ) measurements give  $n$  equations in  $q$  unknown coefficients (fractional delayed neutron yields). The number of time intervals,  $n$ , can be adjusted to suit the precision of the experimental data by appropriate grouping of individual time-channel data from the multichannel analyzer. In the usual case  $n > q$ , standard computer least-squares techniques can be used to obtain best fitted values of fractional delayed neutron yields from measured  $\overline{R}_n$  (and  $\overline{S}_{n/\Delta}$ ) data and the known delayed neutron kinetic functions evaluated at each time channel. This more detailed method of computer analysis of delayed neutron response offers some advantages, including further improvement in isotope discrimination power. For many routine analysis applications, however, the more straightforward  $\overline{R}_f$  method may be generally preferred for its simplicity and operational utility.

#### DELAYED NEUTRON GROUP ENERGY DISCRIMINATION

Based on calculated end-point energies\* for the delayed neutron emission spectra from identified fission product precursors, increased discrimination between fissioning species can be realized by using energy biased neutron detectors (or differential neutron energy spectrometers) in the delayed neutron response measurements outlined above. As expected from fission product  $\beta$ -decay systematics, the shorter delayed neutron periods are associated with higher end-point  $\beta$  energies, and therefore exhibit correspondingly higher-energy delayed neutron spectra. (2) As noted earlier, these shorter period groups exhibit much greater abundance in the long-chain-length (high neutron/proton ratio) fissioning species such

\* Calculated maximum energies,  $E_{n\max} = Q_\beta - B_n$  (see Table 4-11 of Ref. 2), range from 2.04 MeV for  $^{87}\text{Br}$  (55-sec delayed group precursor) to ~5.2 MeV for  $^{140}\text{I}$  (0.5-sec group precursor) and ~9.1 MeV for  $^{93}\text{Br}$  (predicted 0.2-sec group precursor).

as  $^{238}\text{U}$  and  $^{232}\text{Th}$ . The "early" delayed neutrons (e. g., those emitted before  $t = 1$  sec, say) from these long-chain-length species will exhibit a markedly harder energy spectrum than the corresponding early delayed neutrons emitted from the shorter-chain-length species; e. g.,  $^{239}\text{Pu}$  and  $^{233}\text{U}$ . Also, the exceptionally low energy<sup>(2)</sup> of the longest (55 sec) delayed neutron group can be exploited to emphasize characteristic differences in the 55-sec-group relative abundances among the different fission isotopes. Thus, the use of a suitably calibrated energy-dependent detector can provide additional effective isotope discrimination (in nonmoderated or lightly moderated systems) by increasing discrimination factors between the fissioning isotopes. Detailed measurements of individual delayed neutron group spectra for different fission isotopes are being undertaken by the Pulsed Neutron Research Group at Los Alamos.

These spectral measurements--and, in particular, the new energy spectra of the shorter delayed neutron groups ( $i = 4, 5, \text{ and } 6$ )--will permit further refinement and extension of kinetic response methods for identification and analysis based on delayed neutron group energy discrimination.

In its most general (and ultimately most incisive) form, the detailed neutron response method described here involves the determination of delayed neutron time-energy response matrices for each individual fission species. The measured composite response of an unknown system would then be analyzed (viz, by computer methods of matrix inversion) into its component response matrices weighted with fractional delayed neutron yields from each individual fission species. The solutions for relative fission rates, relative amounts of various fissioning isotopes present, etc., are then obtained, as usual, from known  $(\beta\overline{\nu})^q$  and fission cross-section data.

## SUPPLEMENTARY METHODS

High-resolution time-dependent gamma spectrometry can be carried out concurrently with delayed neutron kinetic response methods. For example, lithium-drifted germanium detectors in appropriate coincidence-anticoincidence arrangements may be used to observe well-resolved gamma lines uniquely characteristic of individual fission species in unknown mixtures. One may take advantage of the large yield variations (from one fission species to another) of particular fission product activities to aid in identification of individual isotopes. The greatest sensitivity of fission product yields to  $Z$  and  $A$  of the fissioning species will be found in or near the rapidly varying portions of the fission mass and charge distributions. Although certain characteristic gamma lines can aid in isotopic identification, in general gamma spectrometry cannot compete with neutron techniques for quantitative analysis of different fissioning species in bulk systems; i. e., the very high gamma background in irradiated material and large gamma absorption and self-shielding effects do not provide the required high penetrability afforded by fast neutrons.

Thus, high-resolution gamma spectrometry can provide a useful supplementary isotope-identification technique which, when desired, can easily be carried out concurrently with delayed neutron kinetic response methods for identification and analysis of fissionable isotopes.

## PRACTICAL APPLICATIONS OF KINETIC RESPONSE METHODS

Practical methods of detecting, identifying, and analyzing fissionable material are of obvious importance in the implementation of nuclear safeguards and inspection at both the national and international levels, as well as in many safety, control, regulatory, and surveillance functions of

the atomic energy industry. The high sensitivity of the nondestructive kinetic response methods described herein for discrimination between different fissionable isotopes is perhaps best exemplified by the practical case of  $^{238}\text{U}$ - $^{239}\text{Pu}$  systems, where an effective isotope discrimination factor of  $\sim 5$  can be obtained between  $^{239}\text{Pu}$  and  $^{238}\text{U}$ . (Correspondingly large discrimination factors are obtainable between  $^{233}\text{U}$  and  $^{232}\text{Th}$ .) Thus, the present techniques seem well suited to the assay of  $^{239}\text{Pu}$  or  $^{233}\text{U}$  in power-reactor fuel elements or breeder blanket material, or to rapid nondestructive evaluation of fission isotopic content in irradiated fuel, during fuel reprocessing, fabrication, or any other key point in the nuclear fuel cycle. Similarly, the large effective discrimination factor between  $^{235}\text{U}$  and  $^{238}\text{U}$  enables direct determination of isotopic abundances in enriched uranium fuel elements, ingots, slugs, slurries, melts, solutions, etc.

It is important to note that delayed neutron kinetic response methods constitute a physical sensor of the different fissioning species, and like any sensor, can be calibrated (for given source and detector configuration) to give a direct indication of the absolute amount of each fissionable species present in an unknown system. Thus, for example, reactor fuel elements of different, but known, composition can be used to calibrate delayed neutron isotopic sensor equipment, which can then give directly the absolute amount of each fission species present in fuel elements of the same type but of unknown isotopic composition.

In addition to applications of kinetic response methods to identification and analysis of individual fission isotopes, a further application of considerable practical significance is outlined below. From the data in Figs. 1 to 4 and Tables II, III, and IV, it is clear that maximum discrimination is obtained between two major categories of fission material: the so-called

"special" (fissile) nuclear materials  $^{235}\text{U}$ ,  $^{239(240)}\text{Pu}$ , and  $^{233}\text{U}$  on the one hand, and the "safe" (fertile) nuclear materials, notably  $^{238}\text{U}$  and normal uranium with  $k_{\infty} < 1$ , on the other. This practical distinction between "special" and "safe" nuclear material is fundamental to the field of nuclear inspection, surveillance, and control, which is primarily concerned with the detection and identification of special nuclear material--without necessarily distinguishing, at first, between  $^{235}\text{U}$ ,  $^{239(240)}\text{Pu}$ , and/or  $^{233}\text{U}$ . (More complete isotopic analysis can, of course, be carried out subsequently by more detailed kinetic response methods, if desired.)

The special relevance of kinetic response methods to this important practical problem is apparent from the simple fact that measured delayed neutron response reveals immediately and unambiguously the presence of special nuclear material, as distinct from all other materials, i. e., the unique, tell-tale delayed neutron response from  $^{235}\text{U}$ ,  $^{239(240)}\text{Pu}$ , or  $^{233}\text{U}$ ,

or any combination of these, cannot be duplicated by any other combination of materials, fissionable or nonfissionable. The implications here for both national and future international nuclear safeguards inspection and surveillance methods are clear.

#### REFERENCES

1. Encyclopedic Dictionary of Physics, Vol. 2, "Delayed Neutrons in Nuclear Fission," Pergamon Press, Inc., New York (1961), p. 280.
2. G. Robert Keepin, Physics of Nuclear Kinetics, Addison-Wesley Publishing Company, Inc., Reading, Massachusetts (1965).
3. J. W. Mather, "An Intense Source of Neutrons from the Dense Plasma Focus," in Seminar on Intense Neutron Sources, Santa Fe, N. M., September 19-23, 1966, U. S. Atomic Energy Commission Report No. CONF-660925 (1966), pp. 623-32.